

Contract No:

This document was prepared in conjunction with work accomplished under Contract No. 89303321CEM000080 with the U.S. Department of Energy (DOE) Office of Environmental Management (EM).

Disclaimer:

This work was prepared under an agreement with and funded by the U.S. Government. Neither the U.S. Government or its employees, nor any of its contractors, subcontractors or their employees, makes any express or implied:

- 1) warranty or assumes any legal liability for the accuracy, completeness, or for the use or results of such use of any information, product, or process disclosed; or
- 2) representation that such use or results of such use would not infringe privately owned rights; or
- 3) endorsement or recommendation of any specifically identified commercial product, process, or service.

Any views and opinions of authors expressed in this work do not necessarily state or reflect those of the United States Government, or its contractors, or subcontractors.

Ga_2O_3 : A new class of radiation detector material

Ge Yang, Jacob Blevins

**Department of Nuclear Engineering, North Carolina State
University**

Ralph B. James

Savannah River National Laboratory

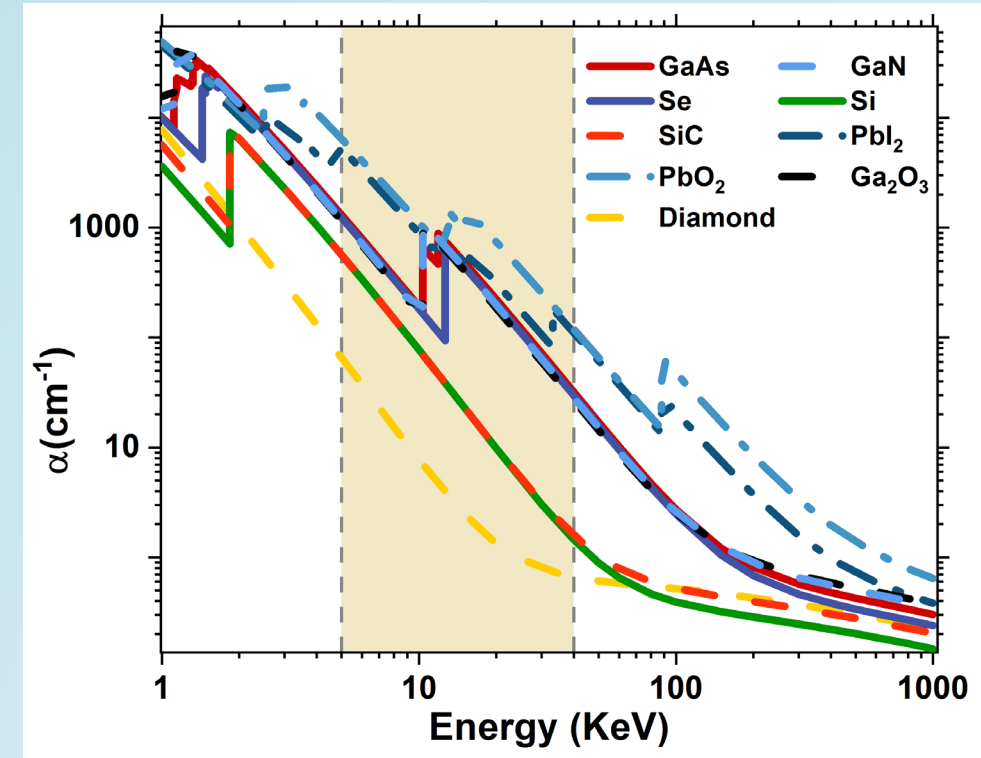
2021 IEEE NSS/MIC/RTSD Conference

Outline

- ❖ Motivation
- ❖ Introduction
- ❖ Optical and electrical characteristics
- ❖ Detector tests
- ❖ Summary

Motivation – A strong need for (U)WBG detectors

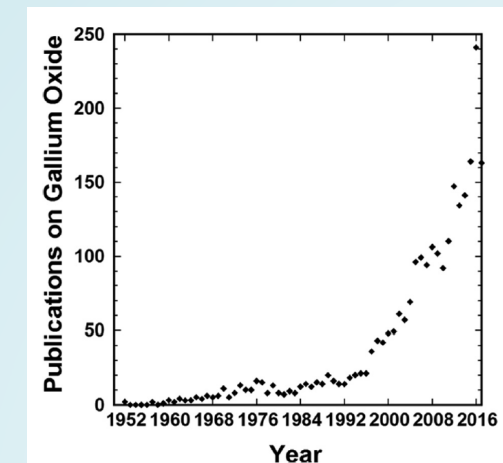
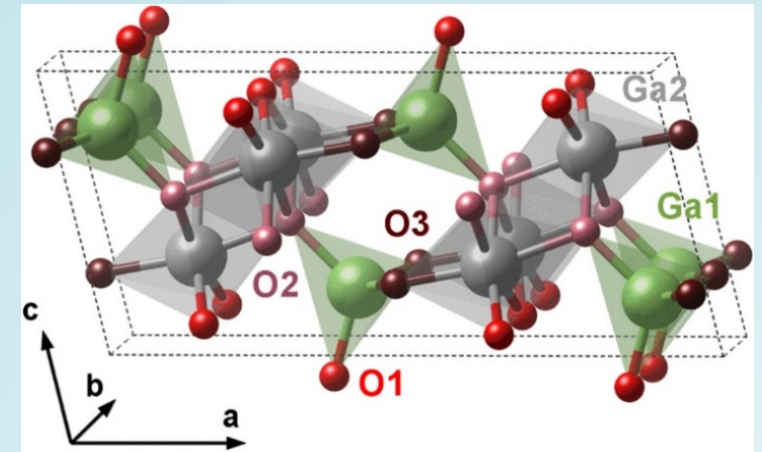
- Radiation detectors are key components for numerous products and applications.
- Elementary detectors have many limitations related to their intrinsic material properties.
 - Harsh environment.
 - Cooling and compromised density.
 - High Voltage operation.
- Wide and ultrawide bandgap semiconductors are much less susceptible to displacement damage by particle irradiation than elemental and narrow bandgap compound semiconductors.



Linear attenuation coefficient of Ga_2O_3 (6.44 g/cm³) compared to several current and candidate X-ray sensing material.

Motivation – Ga_2O_3 for radiation detection

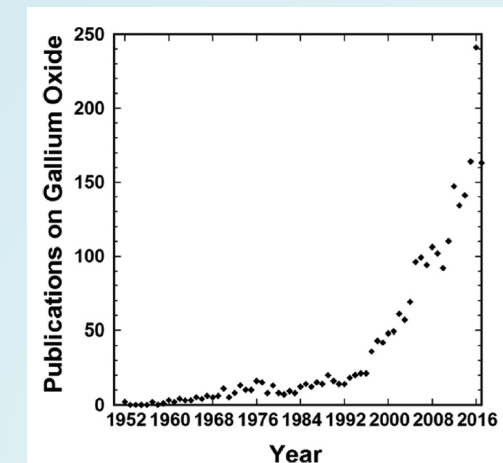
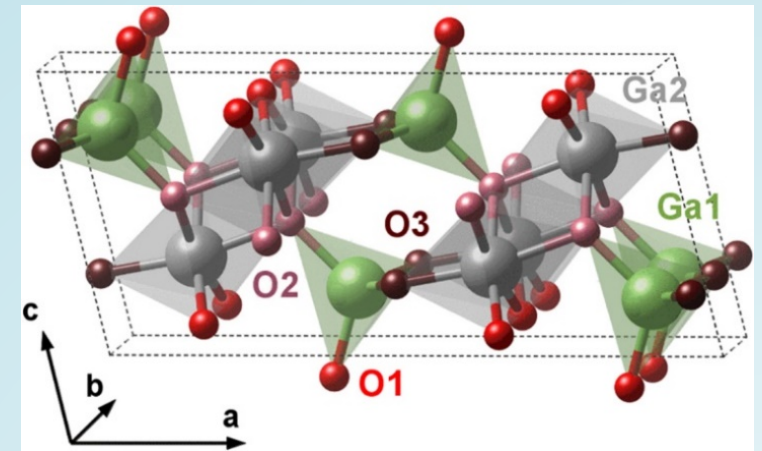
- $\beta\text{-Ga}_2\text{O}_3$ has many material advantages
 - Thermal stability (M. P. > 1800 °C)
 - The least mature and most recent ultrawide bandgap material (4.5 – 5.1 eV)
 - Very high breakdown electric field (8 MV/m)
 - High quality bulk single crystals from melt
 - Cost-effective large-scale manufacturability
- $\beta\text{-Ga}_2\text{O}_3$ holds high promise for fitting many radiation detection application needs not met by currently used materials
 - Harsh environment applicability
 - Versatile and cost-effective synthesis and fabrication
 - High detector performance



S. J. Pearton et al., "A review of Ga_2O_3 materials, processing, and devices," Appl. Phys. Rev., vol. 5, no. 1, p. 011301, Jan. 2018.

Ga₂O₃ properties

- Control of conductivity through doping and mitigation of trap states is key to realizing device applications.
- Mg, N, and Fe compensate n-type conductivity.
- Si, Sn, Ge, F and Cl are n-type dopants.
- Atmosphere dependent post-growth annealing can be used to control conductivity as well (annealing in oxygen reduces the free electron density, while annealing in nitrogen or hydrogen leads to an increase in n-type conductivity).



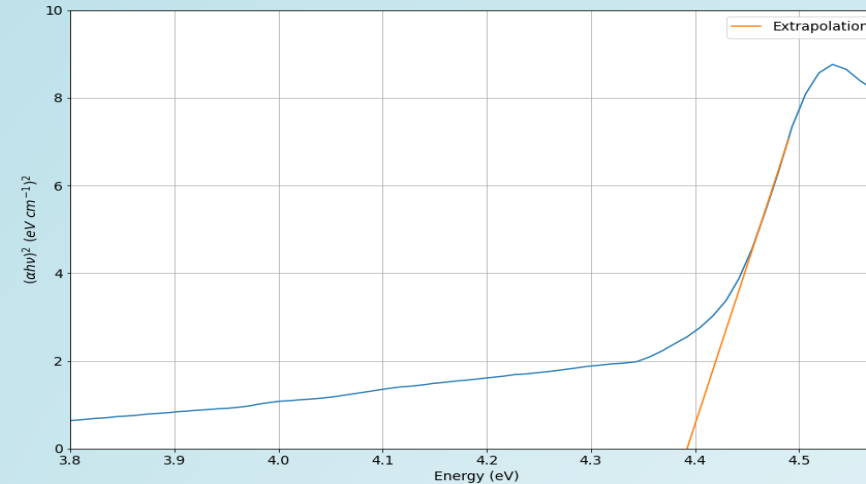
S. J. Pearton et al., "A review of Ga₂O₃ materials, processing, and devices," Appl. Phys. Rev., vol. 5, no. 1, p. 011301, Jan. 2018.

Different Ga_2O_3 samples were used in our study

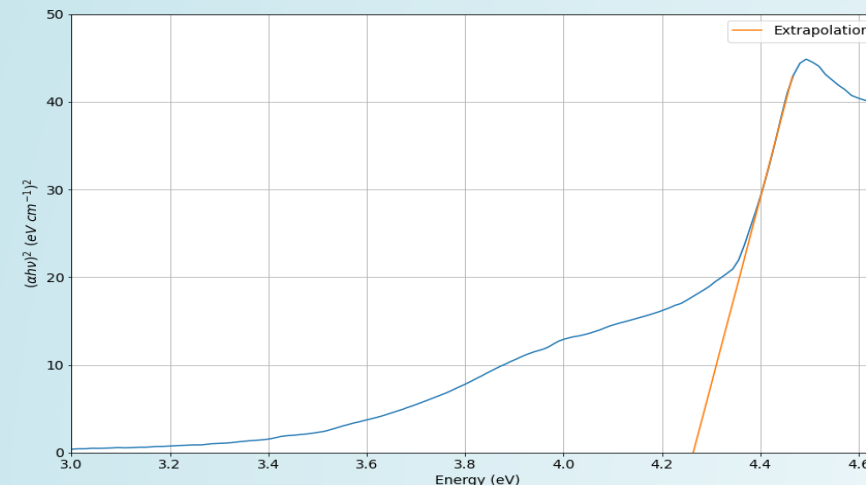
- Ga_2O_3 grown by the floating zone (FZ) method and the edge-defined film-fed growth (EFG) method
- Undoped Ga_2O_3 , Fe-doped Ga_2O_3 and Mg-doped Ga_2O_3

Bandgap Analysis: Mg and Fe doping in FZ samples

- Tauc plots were created from transmission data using a Deuterium-Halogen light source
- The Mg-doped sample has an estimated indirect bandgap of 4.39 eV
- The Fe-doped sample has an estimated indirect bandgap of 4.26 eV
- These band gaps are on the lower end of reported values
- Traditional bandgap values of undoped Ga_2O_3 range near 4.8-4.9 eV
- One possible explanation is high levels of dopants/impurities



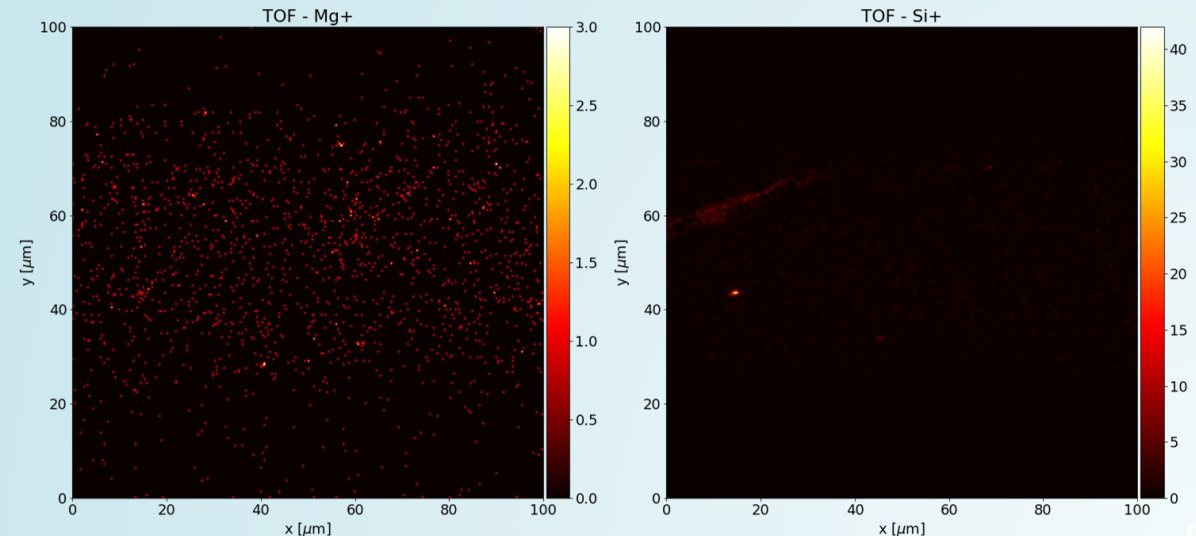
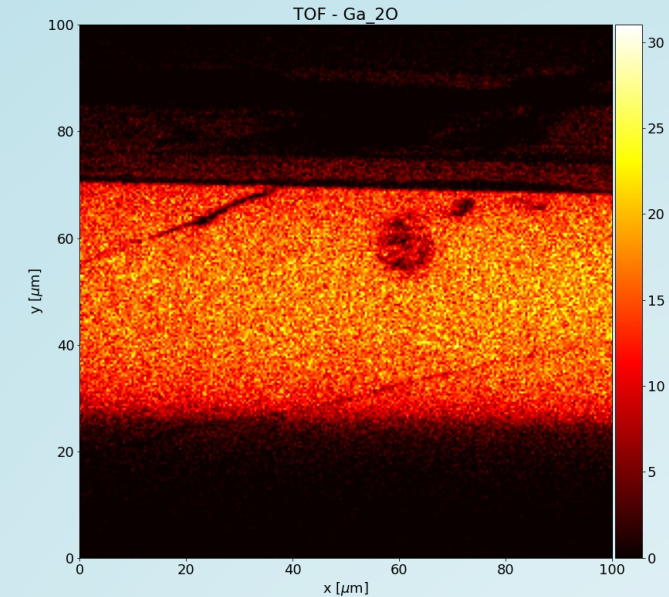
Mg-Doped



Fe-Doped

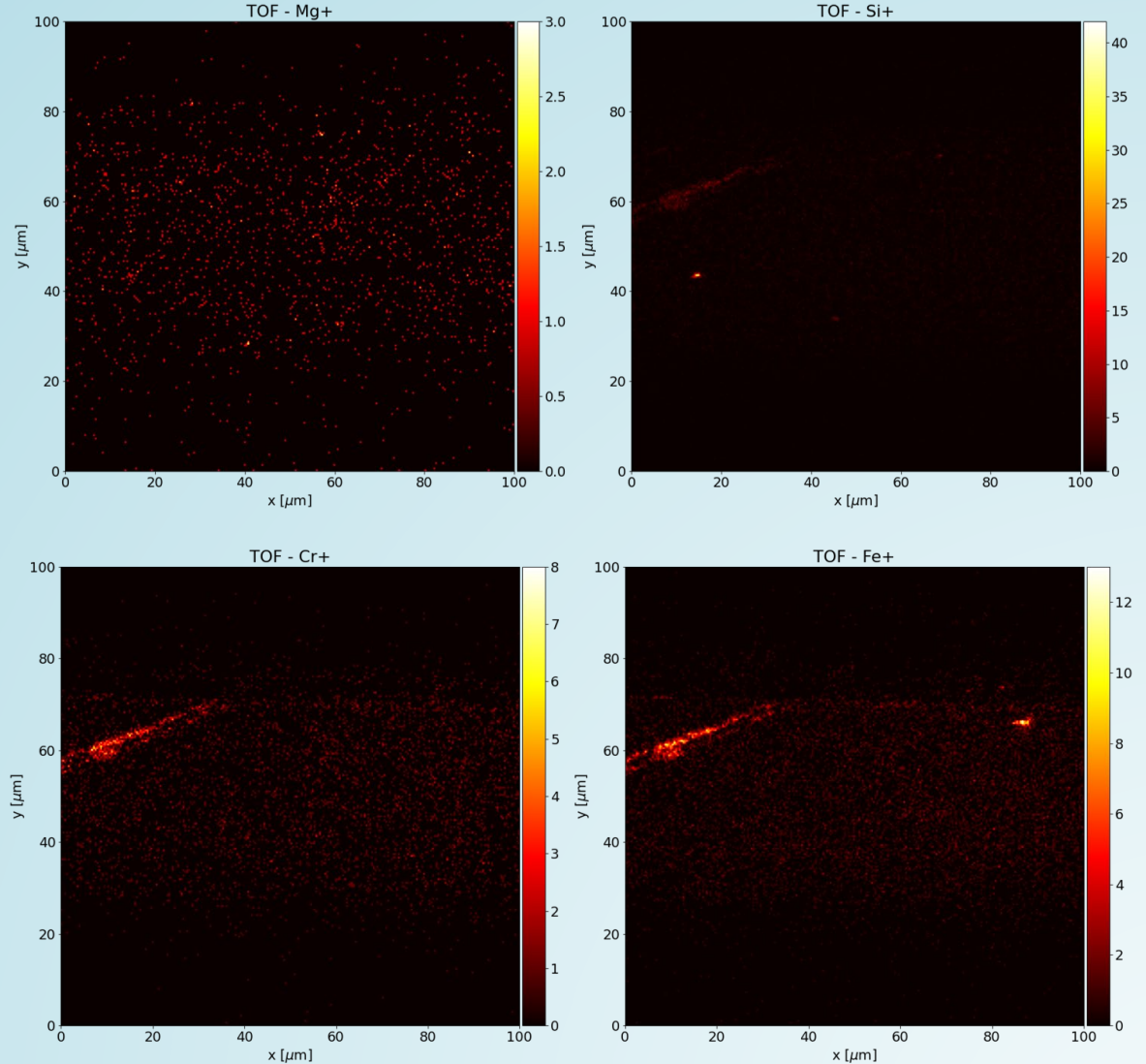
TOF-SIMS: Mg-Doping

- Time of flight - secondary ion mass spectrometry (TOF-SIMS) can be used to observe dopant/impurity distributions within the sample
- The distribution of Mg was uniform across the sampling area
- Direct comparison of dopant/impurity counts from the spectrometer are not appropriate due to different secondary ion potentials
- The presence of Si was also observed, which could be due to the unintentional doping from the raw materials and processing steps



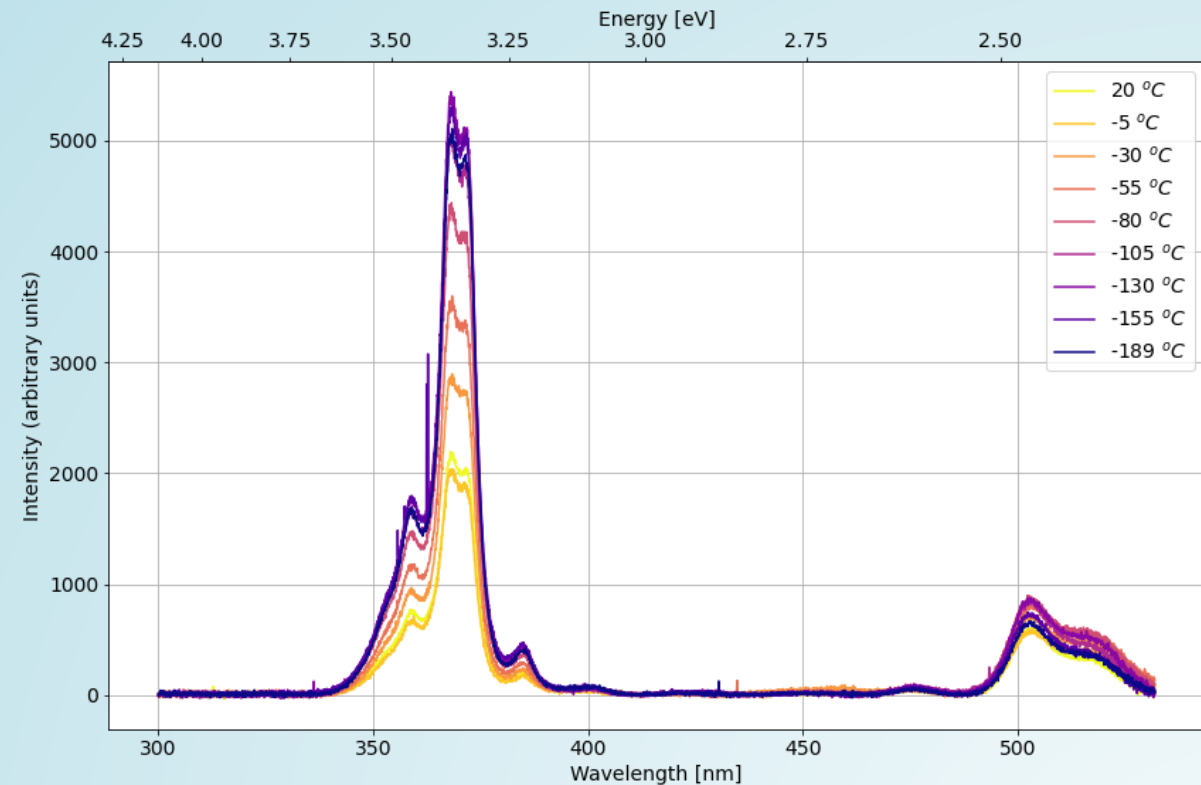
TOF-SIMS: Mg-Doping

- Interestingly there appeared to be higher levels of Cr and Fe at some localized areas
- Note the spatial distributions are different at different locations - especially Si has a hot concentration spot
- These impurity/dopants are important to understand as they could pertain to the cathodoluminescence (CL) results and possible emission mechanisms



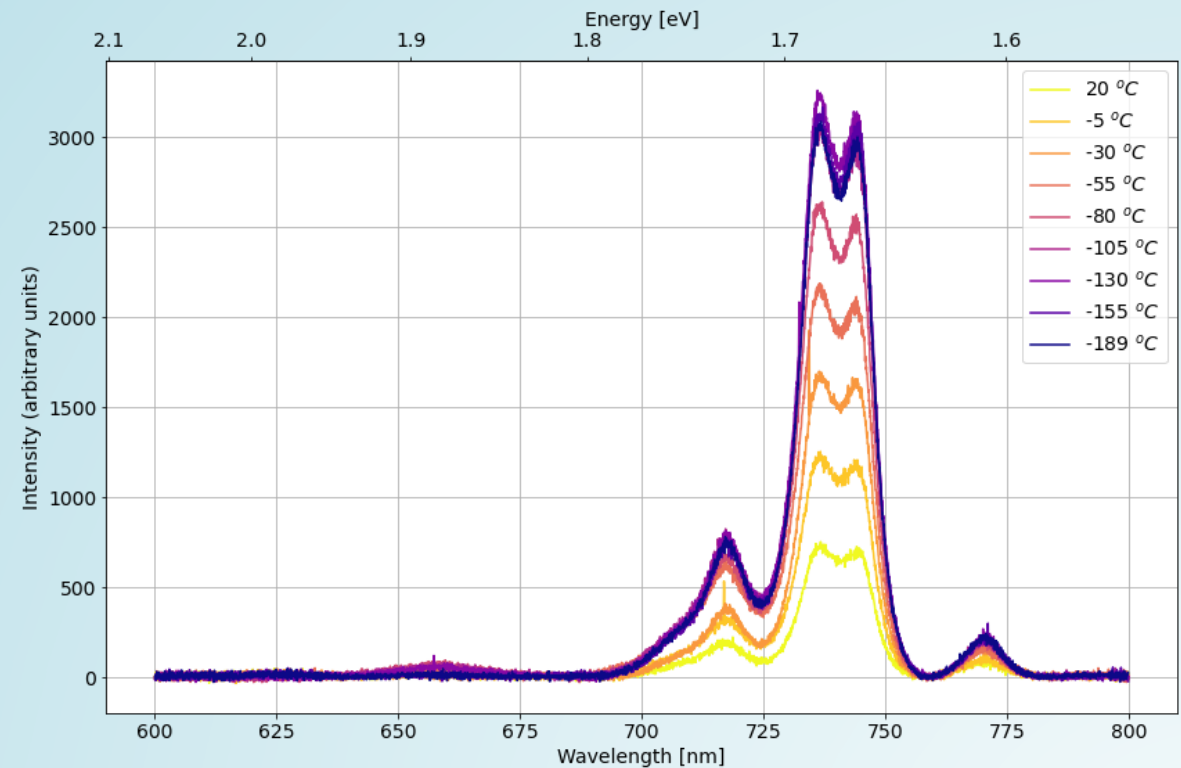
Cathodoluminescence (CL): Mg-Doping

- Beam: 944 pA at 15 keV
- Ga_2O_3 traditionally has a UV blue-green luminescence.
- The origin of the green luminescence ~ 550 nm is not completely clear as many studies report it in undoped samples and others report it only arises through intentional doping with Sn for example.
- Our sample did not emit the traditional broad blue luminescence but did yield green luminescence
- This blue luminescence is believed to result from the recombination from a donor level oxygen vacancy to an acceptor level Schottky defect or gallium vacancy
- Two possible explanations:
 - Another emission mechanism has quenched the blue luminescence.
 - FZ yielded extremely low levels of oxygen vacancies



Cathodoluminescence (CL): Mg-Doping

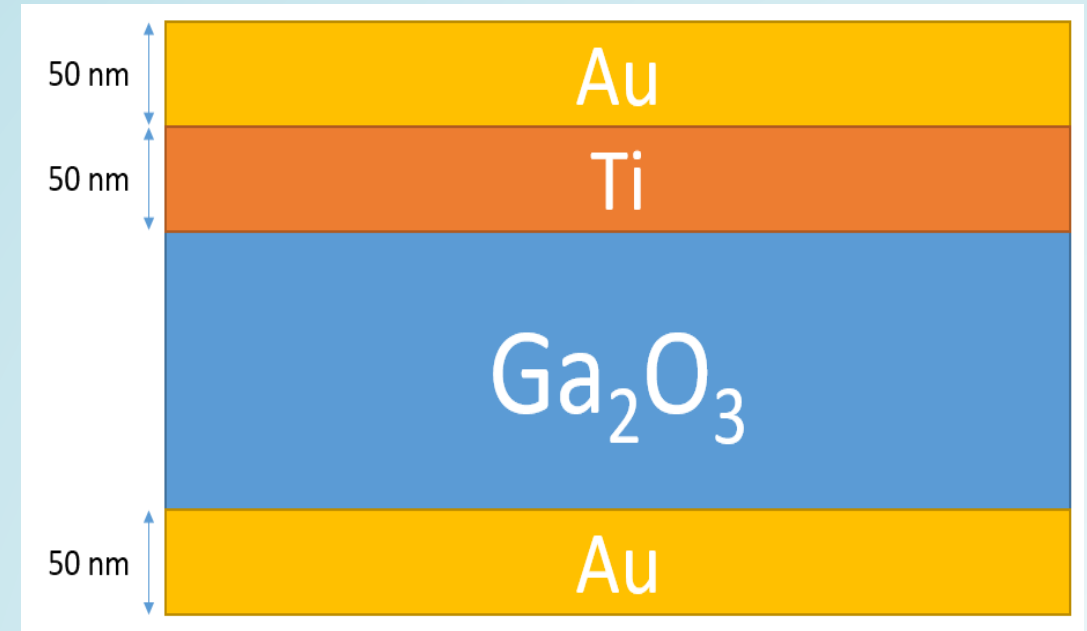
- Undoped Ga_2O_3 does not emit luminescence in the 600-800 nm range. Thus, this should be dopant/impurity driven.
- Similar to the higher energy emissions, all emission peaks increase in intensity down to near -130 °C then drop only slightly in intensity with further decreases in temperature.
- As in the previous figure, every peak increases in intensity to near -130 °C.



Electrode Deposition

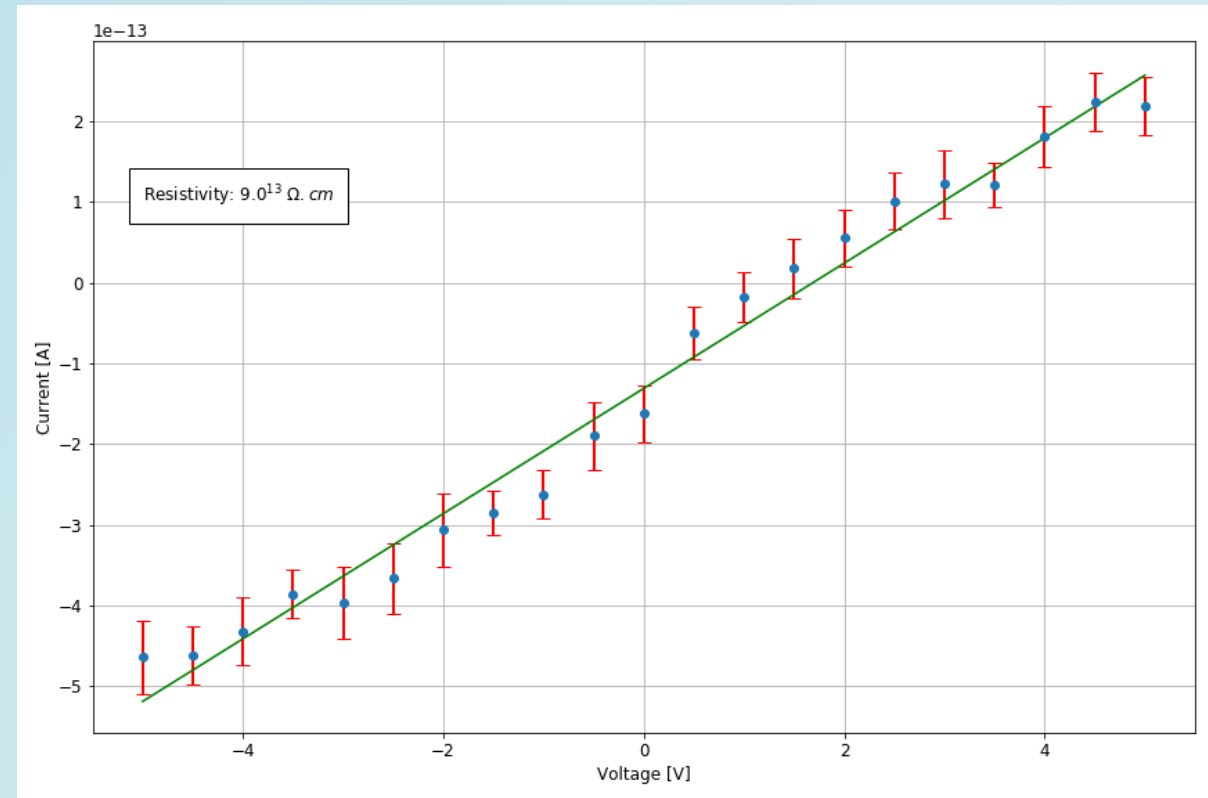
- A vertical sandwich electrode configuration was used for both samples.
- 50 nm for each layer: Au/Ti - Ga₂O₃ - Au
- Based on previous works and the work function of Au, it can produce a Schottky contact with Ga₂O₃.
- To enhance the electrode contacts, a rapid anneal at 400 °C for 1 minute was performed.
- Short annealing times are required as the Ti electrode tends to create a TiO₂ layer for longer anneals, which increases the series resistance.

Vertical Electrode Structure



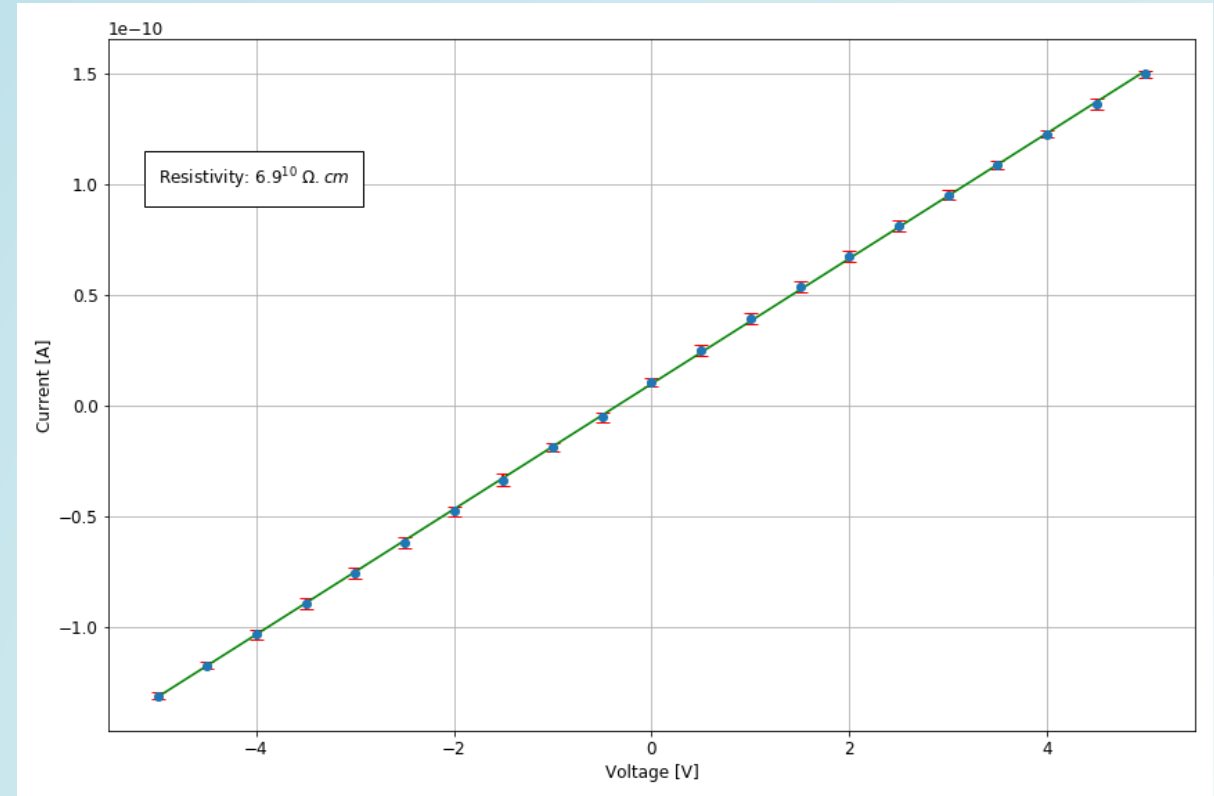
I-V Characteristics: Mg Doping

- Although the Au electrode was expected to create a Schottky diode, the I-V curve still showed some ohmic behavior.
- The Mg doping successfully increased the resistivity far above that of typical undoped samples.
- The resistivity at near $10^{14} \text{ } \Omega\cdot\text{cm}$ allows for the potential of highly sensitive and low-noise radiation detection.
- The I-V curve linearity extended up to 1000 V (system limits).



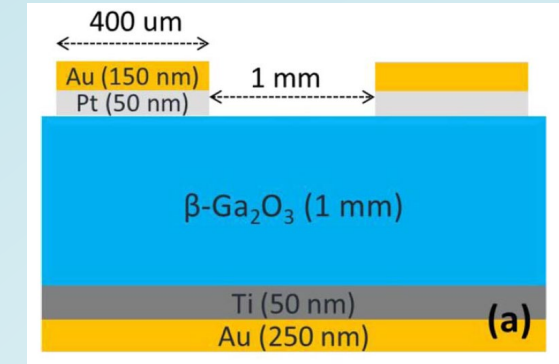
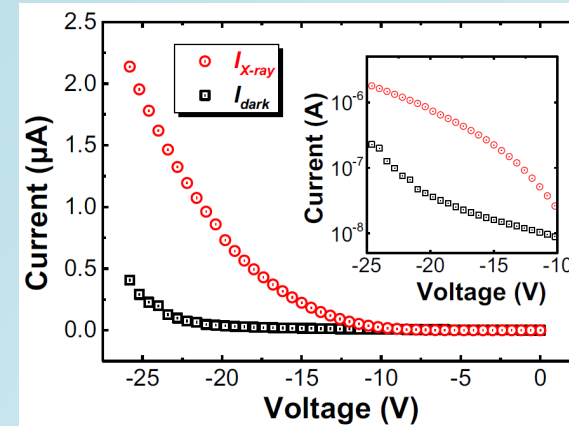
I-V Characteristics: Fe Doping

- Again, the Au electrode did not create a Schottky diode, but the I-V curve showed ohmic behavior.
- Resistivity: $7 \times 10^{10} \Omega \cdot \text{cm}$
- The resistivity is far lower than that of the Mg-doped sample.
- This could be a result of the large amount of unintentional Fe in the Mg-doped sample.
- The I-V curve linearity extended up to 1000 V (system limits).

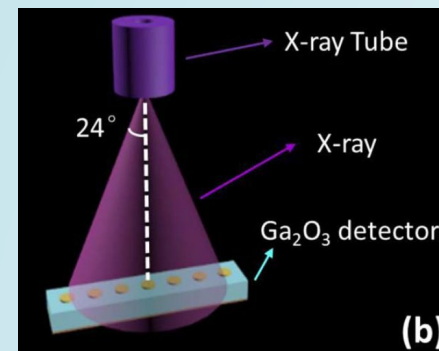


X-ray sensors based on $\beta\text{-Ga}_2\text{O}_3$

- One previous study published in 2018-2019
 - Annealed at 1500 °C in an air atmosphere for 48 hours.
 - Double-side chemical mechanical polishing (CMP).
- Response linearity was demonstrated with no saturation effect.
- High photo-to-dark current ratio exceeding 800 at -15 V .
- When biased at 0V, the detector showed perfect photovoltaic characteristics, demonstrating the great potential of using $\beta\text{-Ga}_2\text{O}_3$ SBDs as passive X-ray detectors or X-ray photocells.



(100) undoped $\beta\text{-Ga}_2\text{O}_3$ EFG based x-ray sensors.

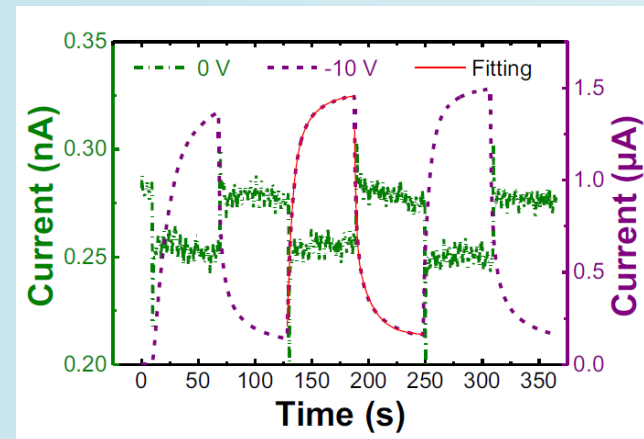
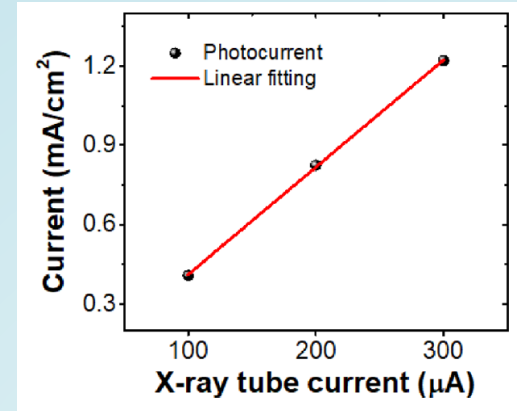


X. Lu et al., "X-ray Detection Performance of Vertical Schottky Photodiodes Based on a Bulk $\beta\text{-Ga}_2\text{O}_3$ Substrate Grown by an EFG Method," ECS J. Solid State Sci. Technol., vol. 8, no. 7, pp. Q3046–Q3049, 2019.

X-ray sensors based on $\beta\text{-Ga}_2\text{O}_3$

- Two different time constants are obtained for the photocurrent rising process ($\tau_{r1} = 13.8$ s and $\tau_{r2} = 1.4$ s), while during the photocurrent decaying process the two time-constants are $\tau_{d1} = 17.1$ s and $\tau_{d2} = 4.0$ s.
- The fast response of an unbiased SBD detector corresponds to a photovoltaic mechanism, where the photo-generated carriers in the space-charge region are swept out rapidly by the built-in electric field.

(100) undoped $\beta\text{-Ga}_2\text{O}_3$ EFG based X-ray sensors. (Lu, 2018)



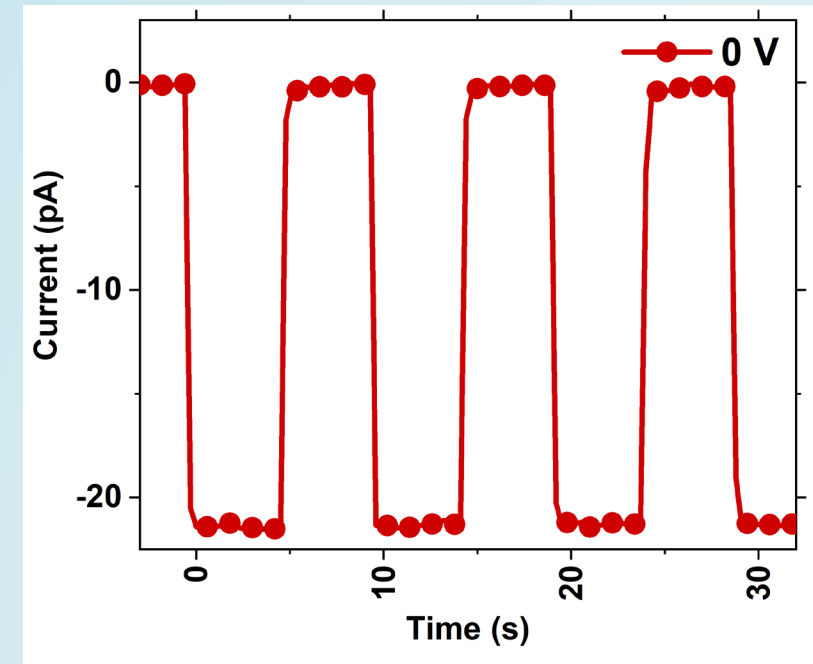
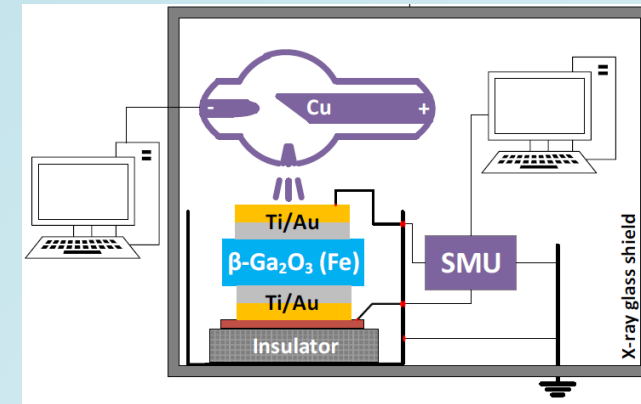
(100) undoped $\beta\text{-Ga}_2\text{O}_3$ EFG based x-ray sensors.

X. Lu et al., "X-ray Detection Performance of Vertical Schottky Photodiodes Based on a Bulk $\beta\text{-Ga}_2\text{O}_3$ Substrate Grown by an EFG Method," ECS J. Solid State Sci. Technol., vol. 8, no. 7, pp. Q3046–Q3049, 2019.

XRIC Characterization of EFG β -Ga₂O₃

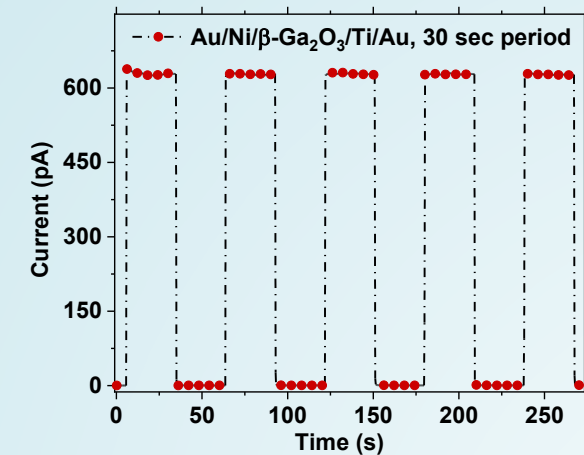
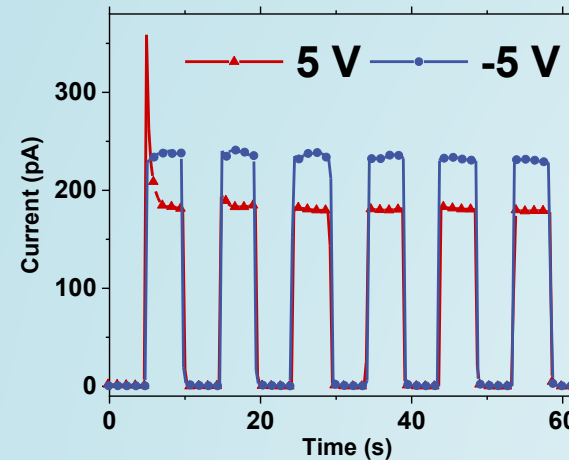
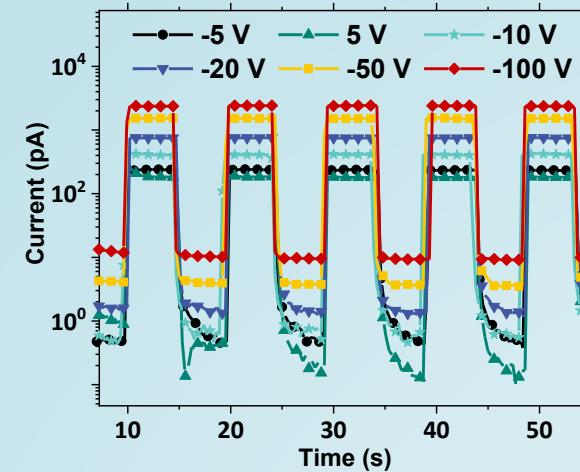
- Zero Voltage mode (Passive operation) (45 KV, 40 mA)
 - X-ray induced current reaching -21 pA
 - Dark transient current of -0.15 (+/-0.05) pA
 - SNR = 139
 - No experimental lag

$$SNR = \frac{I_{x-ray\ induced} - I_{dark}}{I_{dark}}$$



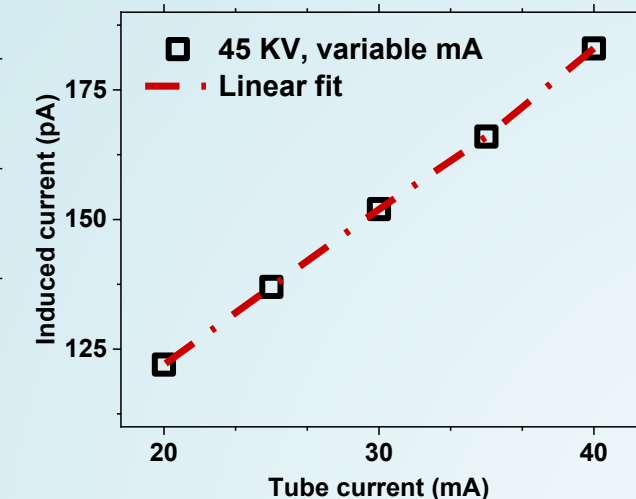
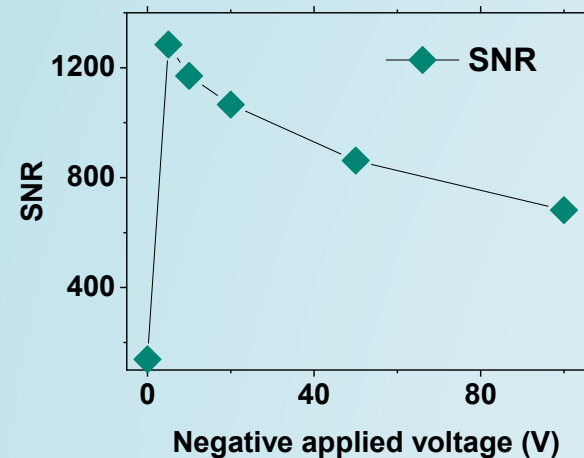
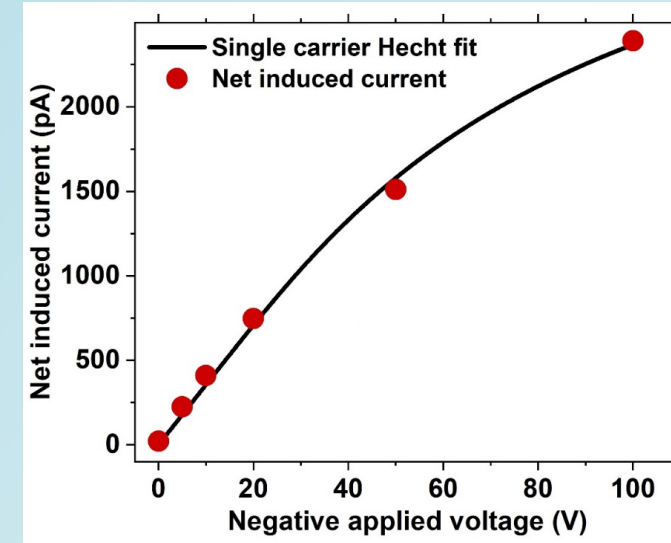
XRIC Characterization

- SNR for operating voltages between -5 V and -50 V stays above 800 and decreases for the higher applied voltages.
- SNR stays above 1000 for applied voltages between -5 V and -20 V, and it is further optimized at -5 V exceeding 1200.
- $\mu\tau$ factor calculated from single carrier Hecht model treatment was $2.28 \times 10^{-5} \text{ cm}^2/\text{V}$
 - 45.6 μm carrier drift length for 10 V.
 - 456 μm carrier drift length for 100 V.



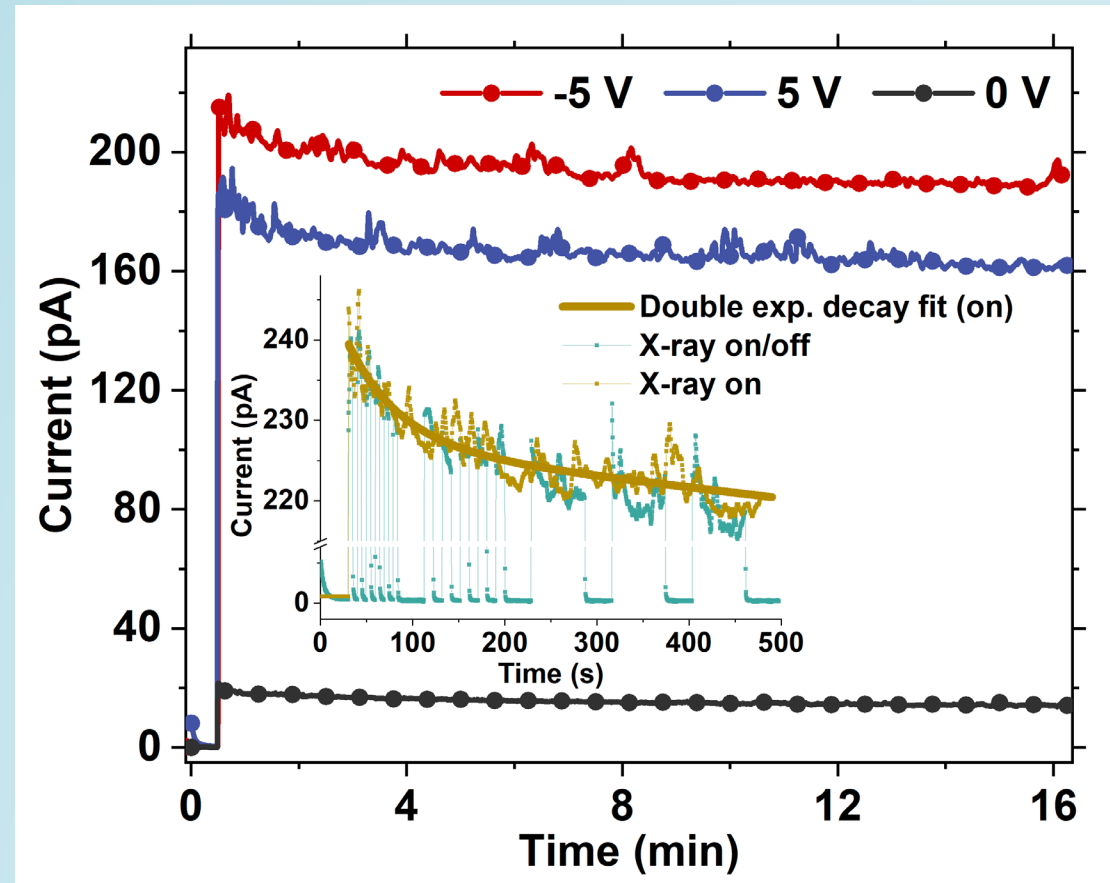
XRIC Characterization

- SNR for operating voltages between -5 V and -50 V stays above 800 and decreases for the higher applied voltages.
- SNR stays above 1000 for applied voltages between -5 V and -20 V, and it is further optimized at -5 V exceeding 1200.
- $\mu\tau$ factor calculated from single carrier Hecht model treatment was $2.28 \times 10^{-5} \text{ cm}^2/\text{V}$
 - 45.6 μm carrier drift length for 10 V.
 - 456 μm carrier drift length for 100 V.



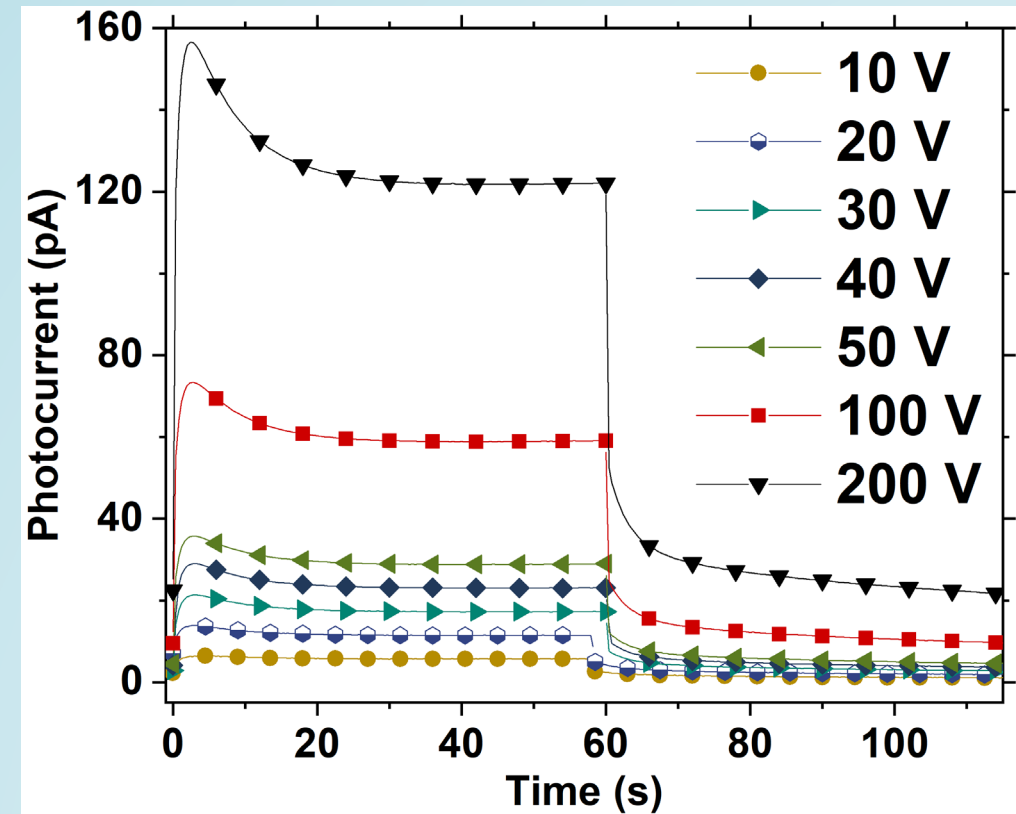
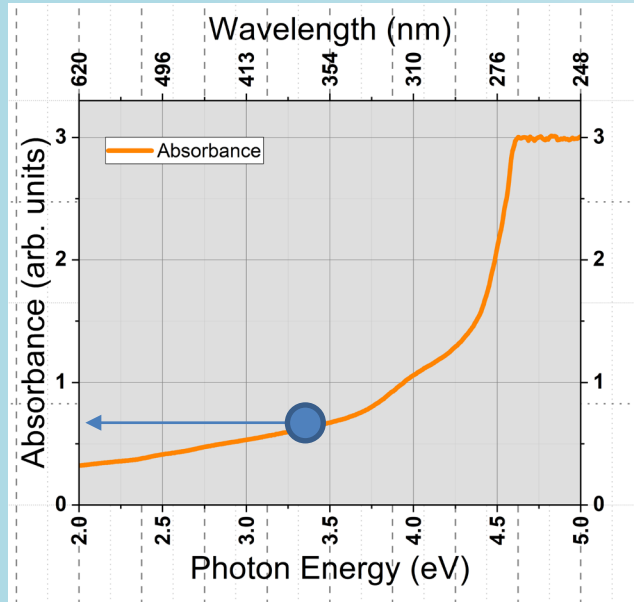
XRIC Characterization

- Highly stable XRIC even at very low operating voltages (5,-5,0 V)
- Small exponential decay within the first minute that stabilizes after that
 - $\tau_1 = 57.7 \text{ sec}$ and $\tau_2 > 10^6 \text{ sec}$, stability
 - Less than 10% decrease in the first minute.
- Operation status independent (for the ON/OFF frequency used)
 - Indicating ion migration and charge accumulation.
 - Slight polarization effect.



UVIC Characterization

- Sub-band gap excitement with 365 nm LED (3.4 eV) was used (band gap of $\beta\text{-Ga}_2\text{O}_3(\text{Fe})$ is 4.45 eV)
- 10%-90% rise/fall time improved from 2 sec/16 sec at 5 V to 1 sec/10 sec at 200 V



Summary

- Ga_2O_3 has been explored as a new radiation detector material.
- CL spectra illustrated the well-known UV emissions but the absence of a broad blue emission. The green and red emissions are believed to be related to dopants/impurities.
- TOF-SIMS showed that Mg and Fe, which could act as acceptors, were both evident in the Mg-doped sample.
- The behaviors of high SNR were investigated under three operation modes for X-ray detection.
- We observed high linearity between X-ray induced photocurrent and X-ray tube current.
- The exciting timing performance of $\beta\text{-Ga}_2\text{O}_3(\text{Fe})$ detectors was demonstrated.
- Our results show that Ga_2O_3 has great potential as a new radiation detector material with excellent temporal response for a wide range of applications.

Acknowledgement

The work is supported by U.S. Department of Energy, Office of Science, Office of High Energy Physics under Award Number DE-SC0021028. We appreciate the discussion with Dr. Aleksey Bolotnikov of Brookhaven National Laboratory. The assistance of Owen Webster and Da Cao is appreciated as well.

Thanks for your attention!